Progress In Electromagnetics Research C, Vol. 22, 35–45, 2011

AN ARTIFICIAL NEURAL NETWORK APPROACH FOR THE HARMONIC DESIGN OF ANNULAR RING DIELECTRIC RESONATOR ANTENNAS

L. Lucci, G. Pelosi, and S. Selleri*

Electronics and Telecommunications Department, University of Florence, Florence 50139, Italy

Abstract—The design and optimization of an annular ring dielectric resonator antenna (DRA) operating in the *C* frequency band is addressed. The DRA is intended to be used as the radiating element of a transmitting array of active integrated antennas, its input impedance must exhibit a proper resistive load at the fundamental resonance frequency, as well as a dominant reactive behavior, either inductive or capacitive, at higher harmonics. The configuration here proposed is a slot-coupled annular DRA where harmonic tuning is performed by resorting to a proper shape factor. The design procedure is performed by exploiting artificial neural networks, to find the resonator geometry starting form the desired resonance frequency, and a finite elements based numerical tool for the electromagnetic characterization of the antenna. Samples of simulation results are shown to demonstrate the capabilities of the proposed slot-based harmonic tuning technique for ring DRAs.

1. INTRODUCTION

In the last two decades wireless technology has determined the development of active integrated antennas (AIAs), a new technology aimed to the integration of planar antennas with active solid state devices to accomplish a number of interesting functions.

In conventional wireless systems antennas and RF front ends (transmitter and/or receiver) are separated blocks interconnected by means of transmission lines or waveguides. Each block is designed as a separate component and the impedance matching to $50\,\Omega$ is required. On the other hand in AIAs the antenna and the active device are

Received 22 April 2011, Accepted 25 May 2011, Scheduled 6 June 2011

* Corresponding author: Stefano Selleri (stefano.selleri@unifi.it).

integrated on a single structure and the antenna operates not only as a radiating element but also as a circuit element (resonator, filter, diplexer) [1].

An advantage of AIAs with respect to conventional antennas is the tight integration between the radiator and the monolithic microwave integrated circuit (MMIC), which results in a smaller device with higher efficiency due to reduced losses in the feeding network, as well as lower production costs.

An AIA system requires the radiator to directly provide the proper load for the power amplifier (PA). In particular the radiator should present an impedance with a real part of a few tens of ohms at the working frequency, (and often also a non-null imaginary part is needed). At the same time, at higher harmonics high purely reactive loads are required to reject radiating modes.

In the literature, many harmonic tuning techniques have been suggested for patch and slot antennas. These techniques are mainly based on the presence of holes, pins, slots or on the shaping of the radiating patch [2–5].

In the last decade, a considerable attention has been focused on dielectric resonator antennas (DRAs) as an alternative to microstrip ones [6–11]. DRAs represent a relatively novel application of dielectric resonators (DRs). These resonators are unshielded and rely, for field confinement within their boundaries, on a very high difference between their own permittivity and the permittivity of the outer medium. The low-loss, high permittivity dielectrics used for DRs ($10 \leq \epsilon_r \leq 100$), ensure that most of the field remains within the resonator, so leading to high quality factor Q. If the permittivity constant is not too high and the excited mode presents strong fields at the resonator boundaries, the Q drops significantly inasmuch part of the stored energy is radiated in the environment. Since dielectric losses remain low and the size of the DR are small with respect to the free-space wavelength, these radiators provide small and high efficiency antennas.

DRAs are used in different applications as they exhibit several attractive features like small size, high radiation efficiency, light weight, simple structure, better performance when used in phased array configurations (since they can be packed more tightly) [12–15]. Furthermore, consisting of 3D structures, DRAs show more degrees of freedom for their geometrical definition and shape [16].

The open literature presents various shapes for DRAs, such as cylindrical (CDRA), rectangular (RDRA), hemispherical (HDRA) and ring or annular DRA (ADRA). Many studies on DRAs have been devoted to radiation efficiency, radiated field characteristics and to enlarge the impedance bandwidth, but less attention has been given to

their harmonic tuning and hence to their use in AIAs. Recently several contributions have been presented where harmonic tuning techniques have been proposed for Ku-band rectangular and cylidrical dielectric resonator antennas [17–19].

This contribution focuses on harmonic tuning of annular DRA operating in C-band. The study has been carried out by exploiting artificial neural networks (ANNs), for the inversion of the formula relating the fundamental resonance frequency and the geometrical parameters of the resonator, and a finite elements based numerical tool (the commercial software HFSS), for the electromagnetic characterization of the antenna.

2. RING DRA GENERALITIES

The general geometry of an anular dielecric resonator is shown in Fig. 1. It consists of a circular cylindrical DRA of radius a and height d, on a metallic ground plane, realized by removing a concentric circular cylindrical core of dielectric material. The parameter b defines the inner radius so that the ratio defined by $\alpha = b/a$ is between zero and unity. Depending on the setting of α, circular cylindrical ($\alpha = 0$) or annular ($\alpha > 0$) DRAs can be formed. Based on the results obtained for a circular cylindrical resonator, we have for the normalised z-component of the generic TM_{npm} electric field inside the resonator:

$$E_z = [AJ_n(k_r r) + BY_n((k_r r))] \left\{ \begin{matrix} \sin(n\phi) \\ \cos(n\phi) \end{matrix} \right\} \cos(k_z z) \tag{1}$$

$$k_r = \frac{X_{np}}{a} \qquad k_z = \frac{(2m+1)/\pi}{2d} \tag{2}$$

$$b \le r \le a, \quad 0 \le \phi \le 2\pi, \quad 0 \le z \le d \tag{3}$$

$$p = 1, 2, 3, \ldots \quad m = 0, 1, 2, \ldots \tag{4}$$

where n is an integer number that depends on the boundary conditions. $J_n(\cdot)$ and $Y_n(\cdot)$ denote the n-th order Bessel functions of the first and second kind respectively. The term $Y_n(\cdot)$ appears when $b > 0$. A and B are arbitrary constants to be determined. X_{np} is the root satisfying the characteristic equation governed by the resonator geometry and boundary conditions. The selection of $\sin(n\phi)$ or $\cos(n\phi)$ depends on the geometry and feed position. In the present geometry, given the position of the slot in the xyz reference (Figs. 1 and 4, the field is maximum at $\phi = 0,\ 180^\circ$ and hence the cosine is to be used. The tuning of the resonator to the desired resonance frequency can be performed acting on several parameters, as the external cylinder radius, a, the internal cylinder radius, b, and the height of the structure, d.

The resonant frequency of the TM_{npm} mode can be derived from the separation equation and has the form [20]:

$$f = \frac{c}{2\pi a\sqrt{\epsilon_r}}\sqrt{X_{np}^2 + \left[\frac{\pi a}{2d}(2m+1)\right]^2} \tag{5}$$

The wavenumber k_r depends on the boundary condition on the inner surface, which can be either metallic or left open. Here we focus on ADRA where inner surface is left open.

To find the field in the ADRA, the inner free-space circular region ($0 \le r \le b$) is modeled using an eigenfunction expansion as

$$E_z = CI_n(k_{0r}r)\begin{Bmatrix}\sin(n\phi)\\ \cos(n\phi)\end{Bmatrix}\cos(k_z z) \tag{6}$$

where C is an arbitrary constant, I_n is the n-th order modified Bessel function of the first kind. In this inner region, the dielectric constant of air is much lower than ϵ_r and the mode is evanescent. As a result the pure imaginary wavenumber is denoted as jk_{0r}. The separation equation becomes:

$$k_z^2 - k_{0r}^2 = \left(\frac{2\pi f}{c}\right) \quad k_{0r}^2 = k_z^2 - \frac{k_z^2 + k_r^2}{\epsilon_r} \tag{7}$$

and k_{0r} is given as

$$k_{0r}^2 = k_z^2 - \frac{k_z^2 + k_r^2}{\epsilon_r} \tag{8}$$

Matching (6) with the expansion (1) across the boundary $r = b$ gives

$$CI_n(k_{0r}b) = AJ_n(k_r b) + BY_n(k_r b) = 0 \tag{9}$$

$$C\frac{k_{0r}}{k_r}I_n'(k_{0r}b) = AJ_n'(k_r b) + BY_n'(k_r b) = 0 \tag{10}$$

By assuming a perfect magnetic wall around the outer circular surface at $r = a$ (6) becomes

$$AJ_n'(k_r a) + BY_n'(k_r a) = 0 \tag{11}$$

and solving the Equations (9), (10) and (11) simultaneously, the characteristic equation will be

$$\begin{aligned} k_{0r}aI_n'(\alpha k_{0r}a)[J_n(\alpha X_{np})Y_n'(X_{np}) + \\ -J_n'(X_{np})Y_n(\alpha X_{np})] + \\ -X_{np}I_n(\alpha k_{0r}a)[J_n'(\alpha X_{np})Y_n'(X_{np}) + \\ -J_n'(X_{np})Y_n'(\alpha X_{np})] = 0 \end{aligned} \tag{12}$$

3. ARTIFICIAL NEURAL NETWORK FOR THE SOLUTION OF THE INVERSE PROBLEM

This contribution focuses on the design of a microwave ring dielectric resonator antenna operating at frequency $f_0 = 5.25\,\text{GHz}$. The annular resonator consists of a dielectric cylinder with a concentric cylindrical cavity. Design mechanical specifications require to have external radius a between 6 mm and 10 mm and height d between 4.5 mm and 7 mm.

The dielectric constant of the material we have considered is $\epsilon_r = 12$, corresponding to silicon.

From the theory the fundamental resonant mode is the TM_{110} whose resonant frequency depends on both geometrical parameters of the resonator and boundary conditions:

$$f_0 = \frac{c}{2\pi a\sqrt{\epsilon_r}}\sqrt{X_{11}^2 + \left(\frac{\pi a}{2d}\right)^2} \tag{13}$$

This frequency is not significantly modified by the two feeding slot dimension, whose effect is mainly seen on the input impedance of the antenna.

Once the resonant frequency has been selected, the dielectric resonator has to be dimensioned by inverting (13), which requires also the inversion of (12).

$$X_{11} = \pi a\sqrt{\frac{4\epsilon_r f_0^2}{c} - \frac{1}{4d^2}} \tag{14}$$

In this work, the inverse problem has been solved by exploiting an artificial neural network approach. The artificial neural network has been exploited to dimension the radiator at the central frequency, and it gives non hints on higher harmonics behavior, hence harmonic tuning is based on a trial and error procedure.

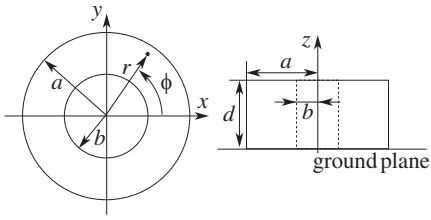

Figure 1. Geometrical parameters defining an ADRA: plane view on the left and side view on the right.

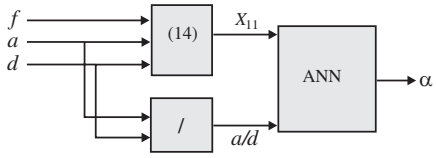

Figure 2. Block scheme of the inversion algorithm.

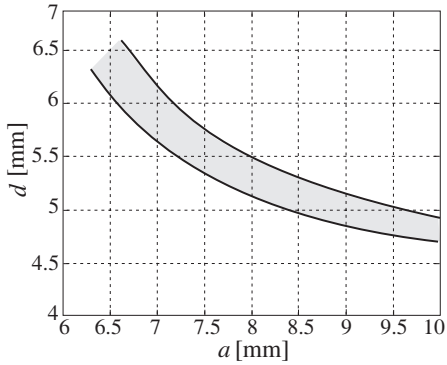

Figure 3. Region of acceptable values for a and d parameters. The region is approximately delimited by two hyperbolas.

In Fig. 2, the block scheme of the inversion algorithm is shown: X_{11} as provided by (14) and a/d parameter are the inputs of the double-layer ANN, with 2 inputs, 1 output, 11 nodes at the first layer and 17 nodes at the second layer. The ANN training procedure has been executed following the backpropagation method [21]. Tansig activation functions were used for the neurons in a Levenberg-Marquardt back propagation training algorithm, lasting 1000 epochs. Learning set comprised 690 samples.

Figure 3 shows the region where design specifications are satisfied, that is where $f_0 = 5.25\,\text{GHz}$, $6\,\text{mm} \leq a \leq 10\,\text{mm}$ and $4.5\,\text{mm} \leq d \leq 7\,\text{mm}$. Within this region 100 configurations, corresponding to 100 couples of values for a and d, have been selected to evaluate the electromagnetic performances of the resonator at fundamental frequency and second and third harmonics.

Numerical analysis has been performed for each selected configuration by means of the commercial software HFSS.

4. ADRA ARCHITECTURE AND HARMONIC TUNING

The antenna model consists of the ring dielectric resonator above a perfect ground plane and electromagnetically coupled with the feeding microstrip via two identical and symmetrical slots realized on the ground plane, Fig. 4.

To better control the S_{11} parameter at the input port, the feeding microstrip ends with a parallel stub, whose length has been varied from 0.5 mm a 4.5 mm with an increasing step equal to 0.5 mm, so as, starting form the 100 possible configurations of the resonator, 900

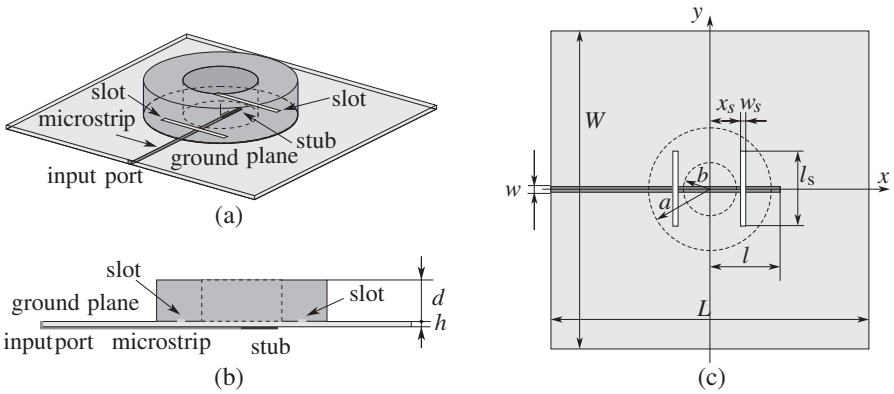

Figure 4. Ring dielectric resonator antenna architecture with microstrip feeding by two identical and symmetrical coupling slots, (a) overall view, (b) side view and (c) real design geometrical parameters.

possible configurations of the antenna system have been studied.

All the 900 configurations have been tested by numerical simulations in the hypothesis of free space operation.

For what concern the antenna behavoir at the fundamental frequency an upper limit of $-10\,\text{dB}$ has been fixed for the S_{11} parameter at the input port. Simulations have been demonstrated that only 75 configurations actually resonate at the desired frequency $f_0 = 5.25\,\text{GHz}$, so that only these configurations have been tested at the second and third harmonics.

To avoid antenna radiation at higher harmonics the condition $S_{11} \geq -2\,\text{dB}$ has been required at second and third harmonics, as this condition assures an acceptable level of antenna mismatch and radiating modes rejection.

Figure 5 shows the S_{11} parameter at fundamental frequency and at second and third harmonics for each of the 75 antenna configurations which resonate at $f_0 = 5.25\,\text{GHz}$. As one can see all configurations have $S_{11} \leq -10\,\text{dB}$ at first harmonic, whereas for about the 40% of the architectures we have $S_{11} \leq -20\,\text{dB}$.

Satisfaction of $S_{11} \geq -2\,\text{dB}$ condition is some more difficult at higher harmonics: in particular for the 75% of the solutions we have $S_{11} \geq -2\,\text{dB}$ at $f = 10.5\,\text{GHz}$ and for only the 36% the same condition is valid at $f = 15.75\,\text{GHz}$.

Among the 75 configurations resonating at $f_0 = 5.25\,\text{GHz}$ a optimal geometry has been selected. The more significant geometrical

parameters of the optimal architecture are shown in Table 1.

In Fig. 6, it is shown the gain of the optimal antenna at first harmonic on the $\phi = 0°$, $\phi = 45°$ and $\phi = 90°$ planes.

The behavior of the optimal architecture in terms of S_{11} parameter is shown in Fig. 7 for (from top to bottom) the first, second and third harmonic.

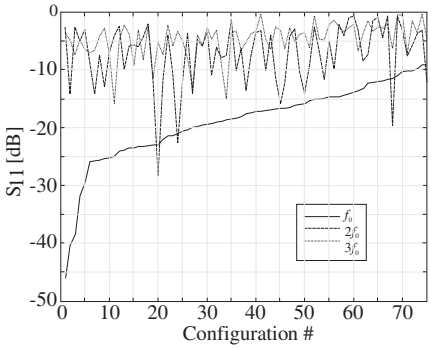

Figure 5. First, second and third harmonic S_{11} parameter for the 75 configurations resonating at the desired frequency $f_0 = 5.25\,\text{GHz}$.

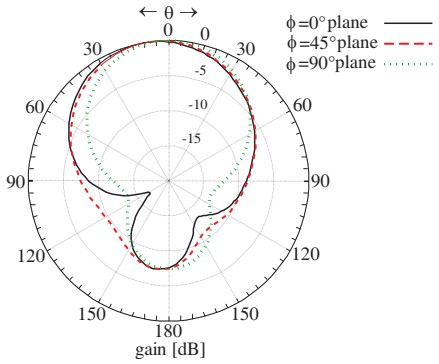

Figure 6. Optimal configuration: gain at first harmonic on the $\phi = 0°$, $\phi = 45°$ and $\phi = 90°$ planes.

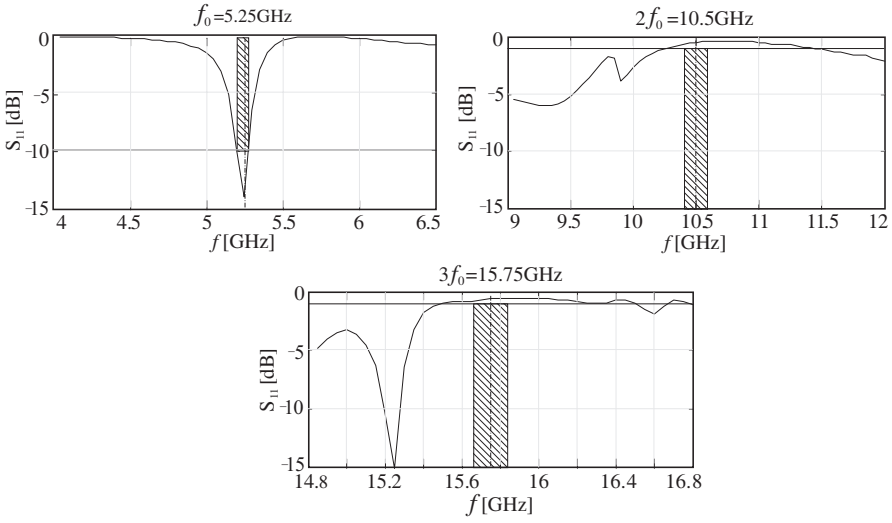

Figure 7. Optimal configuration: input port S_{11} frequency dependance at first, second and third harmonic.

Table 1. Design geometrical parameters.

parameter	[mm]	parameter	[mm]
a	10.000	l	4.844
b	4.785	x_s	3.874
W	30.000	w_s	0.800
L	30.000	l_s	12.636
w	0.483		

5. CONCLUSION

A harmonic tuning technique for a C-band slot-coupled annular DRA has been proposed in this paper. The technique is based on the use of two identical and symmetrical coupling slots instead of the single slot conventionally used in DRA. Some numerical results have been presented to show the effectiveness of the additional slots length as a tuning parameter to control the DRA input impedance at the second harmonic, with a negligible variation of the same impedance at the fundamental frequency. The method proposed does not increase the complexity of the antenna layout with respect to the non-tunable counterpart. Moreover, it has been checked that the radiation pattern characteristics in the principal radiation planes are not significantly influenced by the tuning process.

REFERENCES

1. Chang, K., R. A. York, P. S. Hall, and T. Itoh, "Active integrated antennas," *IEEE Trans. on Microwave Theory and Tech.*, Vol. 50, No. 3, 937–944, 2002.
2. Kim, H. and Y. J. Yoon, "Compact microstrip-fed meander slot antenna for harmonic suppression," *IEEE Electronics Letters*, Vol. 39, No. 10, 761–763, 2003.
3. Kwon, S., B. M. Lee, Y. J. Yoon, W. Y. Song, and J.-G. Yook, "A Harmonic suppression antenna for an active integrated antenna," *IEEE Microwave and Wireless Components Letters*, Vol. 13, No. 2, 54–56, 2003.
4. Kim, H., K. S. Hwang, K. Chang, and Y. J. Yoon, "Novel slot antennas for harmonic suppression," *IEEE Microwave and Wireless Components Letters*, Vol. 14, No. 6, 286–288, 2004.
5. Choi, D. H., Y. J. Cho, and S. O. Park, "A broadband T-shaped microstrip-line-fed slot antenna with harmonic suppression,"

IEEE Microwave Conference Proceedings, APMC, Vol. 4, 4–7, 2005.

6. Zainud-Deen, S. H., H. A. El-Azem Malhat, and K. H. Awadalla, "A single-feed cylindrical superquadric dielectric resonator antenna for circular polarization," *Progress In Electromagnetics Research*, Vol. 85, 409–424, 2008.
7. Si, L.-M. and X. Lv, "CPW-FED multi-band omni-directional planar microstrip antenna using composite metamaterial resonators for wireless communications," *Progress In Electromagnetics Research*, Vol. 83, 133–146, 2008.
8. Al-Zoubi, A. S., A. A. Kishk, and A. W. Glisson, "Analysis and design of a rectangular dielectric resonator antenna fed by dielectric image line through narrow slots," *Progress In Electromagnetics Research*, Vol. 77, 379–390, 2007.
9. Rezaei, P., M. Hakkak, K. Forooraghi, "Design of wide-band dielectric resonator antenna with a two-segment structure," *Progress In Electromagnetics Research*, Vol. 66, 111–124, 2006.
10. Tadjalli, A., A. R. Sebak, and T. A. Denidni, "Resonance frequencies and far field patterns of elliptical dielectric resonator antenna: analytical approach," *Progress In Electromagnetics Research*, Vol. 64, 81–98, 2006.
11. Saed, M. A. and R. Yadla, "Microstrip-FED low profile and compact dielectric resonator antennas," *Progress In Electromagnetics Research*, Vol. 56, 151–162, 2006.
12. Shin, J., A. A. Kishk, and A. W. Glisson, "Analysis of rectangular dielectric resonator antennas excited through a slot over a finite ground plane," *IEEE Antennas Propag. Society Int. Symp.*, Vol. 4, Jul. 2000.
13. Kishk, A. A., "Dielectric resonator antenna elements for array applications," *Proc. IEEE Int. Symp. Phased-Array Syst. Technol.*, 300–305, Oct. 2003.
14. Kishk, A. A., "Experimental study of the broadband embedded dielectric resonator antennas excited by a narrow slot," *IEEE Antennas Wireless Propag. Lett.*, Vol. 4, 79–81, 2005.
15. Mongia, R. K. and A. Ittipiboon, "Theoretical and experimental investigations on rectangular dielectric resonator antennas," *IEEE Trans. Antennas Propag.*, Vol. 45, No. 9, 1997.
16. Petosa, A., A. Ittipiboon, Y. M. Antar, D. Roscoe, and M. Cuhaci, "Recent advances in dielectric-resonator antenna technology," *IEEE Antennas Propag. Mag.*, Vol. 40, No. 35, 35–48, 1998.
17. Guraliuc, A., G. Manara, P. Nepa, G. Pelosi, and S. Selleri,

"Harmonic tuning for Ku-band dielectric resonator antennas," *IEEE Antennas and Wireless Propag. Letters*, Vol. 6, 568–571, 2007.

18. Lucci, L., G. Manara, P. Nepa, G. Pelosi, L. Rossi, and S. Selleri, "Harmonic control in cylindrical DRA for active antennas," *IEEE Antennas and Propagation International Symposium, Conf. Proc.*, 3372–3375, 2007.
19. Lucci, L., G. Manara, P. Nepa, G. Pelosi, and S. Selleri, "Cylindrical dielectric resonator antennas with harmonic control as an active antenna radiator," *International Journal of Antennas and Propagation*, Vol. 2009, 7, Hindawi Publishing Corporation, 2009.
20. Luk, K. M. and K. W. Leung, *Dielectric Resonator Antennas*, Research Studies Press Ltd., Baldock, Hertfordshire, England, 2003.
21. Zurada, J. M., *Artificial Neural Systems*, PWS Publishing Company, Boston, MA, USA, 1992.